Malaysian Journal of Analytical Sciences (MJAS)



Published by Malaysian Analytical Sciences Society

SYNTHESIS AND CHARACTERIZATION OF MAGNESIUM OXIDE NANOPARTICLES BY USING BANANA PEEL (Musa acuminata CAVENDISH) EXTRACT

(Sintesis Hijau dan Pencirian Nanopartikel Magnesium Oksida Menggunakan Ekstrak Kulit Pisang (*Musa acuminata* Cavendish)

Nor Syazwanie Mohd Saidi¹, Kooh Jhi Ying¹, Hanis Mohd Yusoff^{1,2*} and Nurhanna Badar^{1,2}

¹Faculty of Science and Marine Environment, Universiti Malaysia Terengganu, 21030 Kuala Nerus, Terengganu, Malaysia ²Advance Nano-Materials (ANoMa) Research Group, Faculty of Science and Marine Environment, Universiti Malaysia Terengganu, 21030 Kuala Nerus, Terengganu, Malaysia

*Corresponding author: hanismy@umt.edu.my

Received: 18 May 2023; Accepted: 9 August 2023; Published: 30 October 2023

Abstract

The synthesis of metal oxide nanoparticles with the use of plant extract is a promising alternative to chemical synthesis methods. In the study, magnesium oxide nanoparticles (MgO-NPs) were synthesized by using *Musa acuminata* Cavendish banana peel extract solution. The precursor materials used were Mg(NO₃)₂.6H₂O and dried Cavendish banana peel extract solution. Different concentration of Mg(NO₃)₂.6H₂O, different volume of extract solution, and different calcination temperature were used to conduct this study. The green synthesized MgO-NPs were characterized by thermogravimetric analysis (TGA), Fourier transform infrared (FTIR) spectroscopy, ultraviolet-visible (UV-Vis) spectroscopy, scanning electron microscopy (SEM) and x-ray diffraction (XRD). The FTIR spectra showed O-H stretch at 3,340 cm⁻¹ (peel extract solution), 3,308 cm⁻¹/3,348 cm⁻¹ (pre-calcine sample), and 3,086.11 cm⁻¹/3,194.12 cm⁻¹ (calcined at 600 °C). The spectra also showed Mg-O stretching at 655.80 cm⁻¹ and 594.08 cm⁻¹ for pre-calcine and calcined samples, respectively. The wavelength of UV-Vis obtained for 4 sets of green synthesis was around 265 nm due to the surface plasmon resonance band. Thus, confirmed the formation of MgO-NPs. SEM images of MgO-NPs samples showed a mixture of non-uniform sizes and shapes that were agglomerated with average size range of about 90 nm to 320 nm. XRD diffraction analyses displayed the MgO-NPs as a cubic structure.

Keywords: green synthesis, magnesium oxide nanoparticles, Musa acuminata, sustainable materials

Abstrak

Sintesis nanopartikel logam oksida dengan menggunakan ekstrak tumbuhan dapat menjanjikan kaedah alternatif kepada sintesis kimia. Dalam kajian ini, nanopartikel magnesium oksida (MgO-NPs) telah disintesis menggunakan larutan ekstrak kulit pisang *Musa acuminata* Cavendish. Bahan prekursor yang digunakan ialah magnesium nitrat heksahidrat (Mg(NO₃)₂.6H₂O) dan larutan ekstrak kulit pisang Cavendish yang kering. Kepekatan Mg(NO₃)₂.6H₂O, isipadu larutan ekstrak, dan suhu pengkalsinan yang berbeza telah digunakan untuk menjalankan kajian ini. MgO-NPs yang disintesis hijau dicirikan oleh Analisis Termogravimetrik (TGA), Spektroskopi Infra Merah Transformasi Fourier (FTIR), Spektroskopi Ultraviolet-Visible (UV-Vis), Mikroskop Imbasan

Mohd Saidi et al: SYNTHESIS AND CHARACTERIZATION OF MAGNESIUM OXIDE NANOPARTICLES BY USING BANANA PEEL (Musa acuminata CAVENDISH) EXTRACT

Elektron (SEM) dan Pembelauan Sinar-X (XRD). Spektra FTIR telah menunjukkan kewujudan regangan O-H pada 3,340 cm⁻¹ (larutan ekstrak), 3,308 cm⁻¹/ 3,348 cm⁻¹ (sampel sebelum proses kalsin) dan 3,086.11 cm⁻¹/3,194.12 cm⁻¹ (MgO-NPs dikalsinkan pada 600 °C). Spektra FTIR juga menunjukkan regangan Mg-O pada 655.80 cm⁻¹ dan 594.08 cm⁻¹ untuk sampel sebelum dan selepas proses pengkalsinan. Panjang gelombang UV-Vis bagi keempat-empat set adalah pada 265 nm adalah disebabkan oleh jalur resonans plasmon permukaan yang membuktikan pembentukan MgO-NPs. Imej SEM menunjukkan campuran bentuk dan saiz tidak sekata yang teraglomerat dengan anggaran purata saiz sekitar 90 nm hingga 320 nm. Analisis XRD memperlihatkan MgO-NPs sebagai struktur kubik.

Kata kunci: sintesis hijau, nanopartikel magnesium oksida, Musa acuminata, bahan lestari

Introduction

Green chemistry has first been introduced in the America's Pollution Prevention Act of 1990 aiming to reducing pollution at its sources and producing less costly chemical products [1]. According to Murcia et al., there are 12 principles of green chemistry which are waste prevention, atom economy, less hazardous chemical synthesis, designing safer chemicals, safer solvents and auxiliaries, use of renewable feedstocks, reduce derivatives, catalysis, design for degradation, real time pollution prevention, design for energy efficiency and safer chemistry for accident prevention [2]. In synthetic chemistry, green synthesis of nanoparticles, a single-step pollution-free synthesis method [3,4] has been reported to fulfil at least five principles of green chemistry, such as waste prevention, reduce derivatives, safer solvent and auxiliaries, renewable feedstocks and less hazardous chemical synthesis [5]. This production approach is not only environmentally friendly but they are also cost-efficient as well as less toxic [6]. Green synthesis of nanoparticles which employs extracts, such as microorganisms and plant parts like leaves, fruits, and seeds [7] as a reducing and capping agent is a great alternative to the expensive physicochemical methods which poses environmental and biological threat due to the usage of toxic organic solvent and hazardous reagents [8]. Farani et al. has remarked that these natural resources contain biomolecules, polysaccharides, phenolics, vitamins and amino acids which give reducing agent properties to them [9]. Phytochemicals such as terpenoids, aldehyde, carboxylic acids and amides also contribute in the reduction and stabilization [5].

The green synthesis method is broadly used as an alternative to the chemical synthesis method in synthesizing nanoparticles [10]. In the synthesis of

magnesium oxide nanoparticle (MgO-NPs), plants extract such as Embilica officinalis [11], Neem plant [12], Aloe vera [13] and Trachyspermum ammi [14] have been used in the green synthesis as this route replaces the usual conventional physicochemical techniques, such as the sol-gel method, chemical precipitation, and hydrothermal [15]. Fruit waste extract Nepehelium lappaceum L peels [16] Persimmon peels and Citrus aurantium peels have also been used to synthesize MgO-NPs [17, 18]. Although green synthesis of metal oxide nanoparticles by using fruit waste extracts has been extensively studied, the study on biological synthesis specifically for MgO-NPs has not been done widely [19]. The exploration of resources of potential reducing agent is necessary to ensure the efficiency of green synthesis [5].

Magnesium oxide nanoparticles (MgO-NPs) are known to exhibit the ability to withstand extreme conditions and high biocompatibility [20]. MgO-NPs have received a lot of interests for their variety kind of applications [21]. It has been found that MgO-NPs has higher surface to volume ratio and higher surface energy as compared to bulk MgO due to its small particles size [22]. They are evidenced to be great refractory and superconducting materials as they possess good optical and magnetic properties [22]. In biomedicine, MgO-NPs are applied for bone regeneration, relief of heartburns as well as antitumor [23]. They are also known as nontoxic antibacterial agents that is relatively easy to be obtained among all the metal oxide nanoparticles [24]. The properties of the nanoparticles are depending on the size and geometrical structure of the nanoparticles [25]. Therefore, the optimization of reaction conditions, such as volume of extract use, pH value, temperature of reaction, temperature of calcination and volume of starting materials is crucial as these conditions affect the size, shape, form and stability of the nanoparticles produced [26], tailoring the properties of nanoparticles to suit different desired applications.

In this study, Musa acuminata or cavendish banana peel extract was used as reducing and capping agent. Phytochemical tests conducted in previous research showed the presence of secondary metabolite compounds, including alkaloids, flavonoids, saponins, and polyphenols in banana peel extract [27] making it suitable as reducing and capping agent. Previous studies have reported the usage of banana peel extract as a capping agent in the production of metal nanoparticles [28]. Banana peel utilization in the synthesis of ZnO-NPs have also been reported [27,29,30,31,32]. Abdullah et al. [30] in their comparative study of green and chemical synthesis by using cavendish banana peel in the synthesis of zinc oxide nanoparticles (ZnO-NPs) have noted that green synthesized ZnO-NPs exhibited higher crystallinity and smaller particle size. The green nanoparticles synthesized also showed photocatalytic activity comparable to their chemically synthesized counterpart. On this note, green approach is proven compatible to that of chemical approach [30]. The optimization of metal oxide synthesis by using cavendish banana peel has been done as well [29].

While the usage of this peel in metal oxide synthesis has been explored, especially through ZnO-NPs production, the research using banana peel extract are still very limited for MgO-NPs, especially the optimization of synthesis conditions. The study using banana peel extract as reducing agent in the synthesis of MgO-NPs will further explore its potential in metal oxide nanoparticles synthesis. The optimization of conditions by using two different methods with different volume of extracts, different volume of starting materials and different concentration of starting materials were done in this study. MgO-NPs were also produced by calcination with two different temperatures. The study utilizing these parameters is important as they have major impact on the morphology and the biological applications of the nanoparticles produced. Different volume of extracts, mainly determines the yield of nanoparticles [26]. This approach differed from previous study, whereby each parameter was studied

while the others were kept constant [33]. Instead of focusing on the effect of one parameter at a time on the nanoparticles, this study focused on the effect of four parameters concurrently on the nanoparticles. The produced MgO-NPs were characterized by using thermogravimetric analysis (TGA), Fourier transform infrared (FTIR) spectroscopy, ultraviolet-visible (UV-Vis) spectroscopy, scanning electron microscopy (SEM) and X-ray Diffraction (XRD) to further understand the effects of parameters on the size, surface morphology and crystallite structure of MgO-NPs.

Other than that, the utilization of the peel which contributes to a major agriculture waste [34] allows the researchers to harness renewable feedstocks as well as preventing waste and derivatives that align with the principles of green chemistry. By using banana peel as reducing agent, the researchers manage to provide safer chemicals and solvents which is better to the people and environment. In the synthesis methods, low temperature and short reaction time were operated allowing efficient energy consumption and high feasibility. Hence, the usage of banana peels extract is considered environmentally, socially and economically sustainable, making it a 'green' approach.

Materials and Methods

Materials

Magnesium nitrate hexahydrate (Mg(NO₃)₂) were purchased from Sigma Aldrich and used without further purification. *Musa acuminata* Cavendish bananas were brought from local supermarket in Petaling Jaya, Selangor. Distilled water was used to prepare all the solutions and Whatman No. 1 filter paper was used to filter MgO-NPs solution.

Synthesis of magnesium oxide nanoparticles (MgO-NPs): Preparation of banana peel extract

The *Musa acuminata* Cavendish banana peels were rinsed thoroughly with distilled water and cut into smaller pieces. The peels were oven dried at 150 °C for 4 h and ground into powder. A total of 20 g powdered banana peel was added in a beaker with 200 mL of distilled water. The mixture was heated at 70 °C–80 °C for 1 h and filtered with filter paper. Excess extract solution was kept in the refrigerator (maximum 24 h).

Phytochemical tests of banana peel extract

To investigate the compounds presence in the banana peel extract, several phytochemical tests were carried out. This included saponin test, alkaloid test, tannin test, phenol test, flavonoid test, terpenoid test, and glycoside test. Table 1 shows a list of methods for each test. Each test was performed at least three times and only tests which appeared positive in two or more tests were considered to confirm the presence of the active compounds in banana peel extract.

Table 1. Phytochemical tests methods.

Tests	Methods
Saponin Test	1 mL of peel extract solution was added with 2 mL of distilled water in a test tube. The solution was shaken vigorously and was observed for a stable persistent froth for 10 min.
Wagner's Test	0.5 mL of peel extract solution were treated with a few drops of Wagner's reagent (iodine in potassium iodide). The colour changes were observed, and a brown precipitate formed to indicates the presence of alkaloid.
Mayer's Test	0.5 mL of peel extract solution was treated with a few drops of Mayer's reagent (potassium mercuric iodide). A yellow cream precipitate formed to indicates the presence of alkaloid.
Tannin Test	0.5 mL of peel extract solution was added with 1 to 2 drops of 10% iron (III) chloride solution. A dark green or blue-green coloration indicates the presence of tannins.
Phenol Test	0.5 mL of peel extract solution was put into test tube was added followed with 2 to 3 drops of 10% iron (III) chloride solution. The presence of green or blue colour indicates the presence of phenolic compound.
Flavonoid Test	0.5 mL of peel extract solution was treated with few drops of concentrated sulphuric acid. The colour changes were observed, and a formation of orange colour indicates the presence of flavonoid.
Salkowski Test	$0.5~\text{mL}$ of peel extract solution was added with $2~\text{mL}$ of chloroform followed by $3~\text{mL}$ concentrated H_2SO_4 carefully to form a layer. Terpenoids are present if a reddish-brown colouration is observed.
Liebermann's Test	3 mL of peel extract solution was added with 2 mL of CHCl ₃ and 2 mL of CH ₃ COOH. A blue colour solution changes into green colour indicated the presence of glycosides.

Green synthesis of magnesium oxide nanoparticles (MgO-NPs)

MgO-NPs were synthesized with two different set of conditions, (A) 30 mL peel extract with 150 mL Mg(NO₃)₂ (0.05 M) aqueous solution; (B) 25 mL peel extract with 200 mL Mg(NO₃)₂ (0.10 M) aqueous

solution. An amount 30 mL of banana peel extract was added to 150 mL of $Mg(NO_3)_2$ (0.05 M) aqueous solution. The reaction mixture was stirred at a constant temperature of 80 °C by using a magnetic stirrer hot plate for 2 h. Color changes were noted for the reaction mixture as it indicates the formation of precipitate.

After the 2 h of constant stirring and heating, the mixture was cooled down to room temperature. The cooled mixture was centrifuged at 8,000 rpm for 20 min. The mixture was filtered and oven dried at 80 °C overnight. The fully dried precipitate was ground with mortar and pestle.

Thermogravimetric analysis (TGA) was conducted prior to calcination to determine the suitable calcination temperature. To obtain the final product, MgO-NPs, the ground samples from previous step were calcined in the furnace at the suitable temperatures for 5 h. The procedure was repeated with Condition B.

Characterization of magnesium oxide nanoparticles (MgO-NPs): Thermogravimetric analysis (TGA)

Perkin Elmer Pyris 6 TGA thermogravimetric analyzer was used to quantitatively monitor the weight change in the sample as a function of temperature. About 5 mg of pre-calcine MgO-NPs were weighed and used on each analysis to avoid any influence of sample quantity in the analysis. The analyses were performed in the presence of nitrogen gas with a constant flow rate of 20 mL min⁻¹ throughout the process. The analyses were conducted within temperature range of 30 °C to 900 °C at a ramping rate of 10 °C min⁻¹. The TGA graph were obtained after the analyses.

Fourier transformation infrared (FTIR) spectroscopy

The FTIR analyses were performed by using Shimadzu model IRTracer-100 spectrophotometer in the range of 400 cm⁻¹ to 4,000 cm⁻¹ with the attenuated total reflectance (ATR) technique. The diamond on the sample platform was cleaned with acetone by using lens paper. A background scan without any sample on the diamond was done. A small amount (about 5 mg) of precalcine MgO-NPs were placed on the diamond until it was fully covered for each analysis. The pressure arm was placed into position and locked over the diamond filled with sample. Force was applied on the sample, pushing it onto the diamond surface. Finally, the sample was analyzed with the software and the FTIR spectra were obtained.

Ultraviolet-Visible (UV-Vis) spectroscopy

Shimadzu UV-Visible spectrophotometer model UV-1800 was utilized for the characterization of MgO-NPs. The baseline was set with the blank. The reference cuvette and measurement cuvette were filled with distilled water. The cuvettes were placed and aligned properly in the spectrometer. After setting the baseline, the measurement cuvette was removed and rinsed twice before filling with sample. The cuvette was ensured that it was clear from fingerprints and placed into the spectrometer for analysis. The wavelength range of the analyses were set to be within 200 nm to 800 nm with a resolution of 1 nm. The absorbance spectra were collected after the analyses.

Scanning electron microscopy (SEM)

The morphology of MgO-NPs samples was analyzed from the images generated from the TESCAN VEGA scanning electron microscope. To prepare the samples, double-sided carbon adhesives were applied onto the SEM stubs and the protective films were removed.

Then, the MgO-NPs samples were placed on the adhesives and coated them with gold (Au) by using the gold sputtering machine. The coated samples (on the stubs) were loaded onto the sample stage in the SEM chamber. Then, suitable spots for desired structure or morphology of MgO-NPs were located and the SEM images were captured at 4 magnifications, 5kx, 10kx, 15kx, 20kx.

X-ray diffraction (XRD)

To identify phases and patterns of MgO-NPs, XRD analyses were conducted by using Rigaku Miniflex II diffractometer (30 kV, 15 mA) with Cu K- α radiation (1.5418 Å) with a Bragg's angles, 20 range of 20° to 80° with a scan rate of 2°/min.

The MgO-NPs samples were ground by using agate mortar and pestle to produce a uniform fine powder. The samples were placed onto a glass sample holder with a square hollow-ground side. The excess samples were cleared by sliding across the sample holder with a glass plate. Then, the surface of the samples was smoothed with the back of the glass plate. Any excess samples on the glass sample holder (around hollow-ground side) were wiped off. The sample holder was carefully

inserted onto the sample holder slot, ensuring no sample spills for the XRD analyses.

Results and Discussion

Several phytochemical tests were conducted on the Cavendish banana peel extract solution to confirm the bioactive compounds and the functional groups responsible for the reduction and capping of MgO-NPs. Table 2 shows that alkaloid, tannin, phenol, flavonoid, and terpenoid were present in banana peel extract solution.

The phytochemical tests were carried out in triplicate and labelled as 1, 2, and 3 for each compound to confirm the consistency and accuracy of the results. The presence of the compound of interest in the peel extract solution will only be considered if two or more positive results were obtained from the tests. The findings were mostly similar to previous studies [27, 35], however with a slight difference. In their studies, saponin and glycoside were present in banana peel extract solution while it was not present in this study. The different outcomes could be due to the drying condition of the banana peels [36].

Table 2. Phytochemical test results of Cavendish banana peel extract solution

	Tests	1	2	3
Saponin	Foam Test	-	-	-
Alkaloid	Mayer's Test	+	+	+
Aikaioiu	Wagner's Test	+	+	+
Tannin	Ferric Chloride Test	+	+	+
Phenol	Ferric Chloride Test	+	+	+
Flavonoid	Flavonoid Test	+	+	+
Terpenoid	Salkowski's Test	+	+	+
Glycoside	Liebermann's Test	-	-	-

Note: (+): detected, (-): not detected

Thermogravimetric analysis (TGA)

Thermogravimetric analyses were carried out to determine the suitable temperature for calcination of the green synthesized MgO-NPs [37]. Figure 1 shows the thermogravimetric graph of two pre-calcined samples with two different sets of volume and concentration of starting materials. Based on Figure 1, the initial stage of weight loss below 100 °C was due to the evaporation of moisture and other volatile compounds [38], whereas the weight loss started at below 550 °C was due to the decomposition of the phytochemical compounds in peel extract and other organic compounds [37,39].

TGA curve for the MgO samples showed that weight loss of almost 87% from 30 °C had occurred continuously up to 600 °C as the graph showed almost a plateau thereafter. This indicated that MgO-NPs synthesized by using Method A and Method B were

thermally almost stable starting at 600 °C and continuing up to the maximum temperature of 900 °C [39]. From this information, the green synthesized precalcine samples were subjected to calcination at 600 °C and 800 °C. It can be concluded that the formation of MgO synthesized with both Condition A and Condition B took place with heating at more than 600 °C.

Fourier transformation infrared (FTIR) spectroscopy

FTIR results were obtained for MgO-NPs synthesized with Condition A are shown in Figure 2, the broad peak centered at (a) 3340.71 cm⁻¹, (b) 3308.85 cm⁻¹, and (c) 3086.11 cm⁻¹ were due to the stretching vibration of O-H group [38,39]. The presence of O-H groups is supported by the absorption peak at (a) 1635.64 cm⁻¹ and (b) 1620.21 cm⁻¹, which corresponded to the bending mode of O-H bond [18].

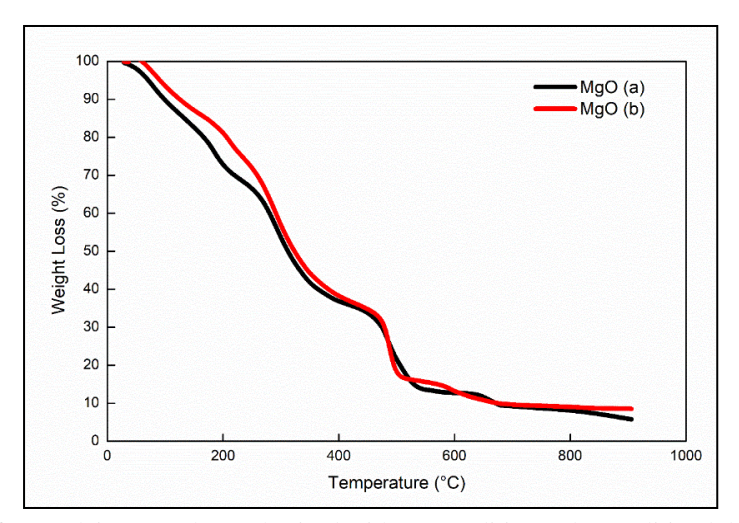


Figure 1. TGA graph of pre-calcine sample synthesised with (a) condition a (b) condition b before calcination.

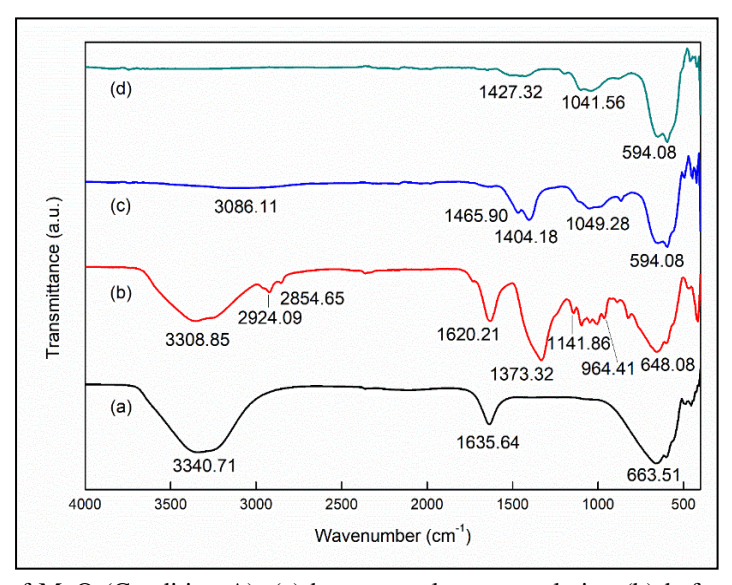


Figure 2. FTIR Spectra of MgO (Condition A): (a) banana peel extract solution (b) before calcine; (c) calcined at 600 °C; (d) calcined at 800 °C

The O-H groups located around 1630 cm⁻¹ could be from the hydroxyl groups of the phytochemical compounds in the peel extract that were involved in the capping reaction [39]. Overall based on Figure 2 (b), Figure 2 (c) and Figure 2 (d), both O-H peaks became narrower and eventually disappeared with increasing calcination temperature as elimination of water molecules in the samples increased [40].

Other than O-H stretching, the broad peak centered at (a) 3340.71 cm⁻¹ could also be the stretching vibration

of N-H groups, which is a feature of phenolic compounds, such as glycosides, tannins, and flavonoids [41]. This finding agreed with the phytochemical test result conducted. Moreover, the two small absorption peaks at 2924.09 cm⁻¹ and 2854.65 cm⁻¹ shown in Figure 2 (b) represented the C-H stretching vibration in CH₂ groups which could be due to the phytochemical compounds [42]. The peaks slowly became indistinguishable as the calcination temperature increased. This meant that the capping reaction with phytochemical compounds had occurred [43].

The absorption peak at (b) 1373.32 cm⁻¹ represented the C-H bending vibration. Whereas the peaks at (c)1404.18 cm⁻¹ to 1465.90 cm⁻¹ and (d) 1427.32 cm⁻¹ were assigned to Mg-H which indicated the formation of hydride ion [44]. Besides, absorption peaks located between (b) 964.41 cm⁻¹, and 1141.86 cm⁻¹ were most likely attributed to C-O and C-O-C diagnostic bonds [42]. The peaks at 2924.09 cm⁻¹ and 1141.86 cm⁻¹ in Figure 2 (b) proved the presence of polysaccharides, polyphenols and proteins [38] as the peaks corresponded to the functional groups contained in those phytochemicals in the pre-calcined MgO-NPs. The peaks became narrower when the samples were calcined, indicating that possibly the phytochemicals had undergone capping reaction.

The appearance of extra peaks at 3086.11 cm⁻¹, 1465.90 cm⁻¹, 1404.18 cm⁻¹, 1049.28 cm⁻¹ and (d) 1427.32 cm⁻¹, 1041.56 cm⁻¹ might be due to: (1) formation of crystalline inorganic compounds present in the peel extract during the calcination process; and (2) strong bonds that stabilized the formation of MgO-NPs after the decomposition of phytochemicals which remained over the surface of MgO-NPs [41]. The broad absorption peaks at (b) 648.08 cm⁻¹ and (c, d) 594.08 cm⁻¹ from all FTIR spectra obtained for green synthesized MgO-NPs with Condition A, indicated the stretching vibration mode for the Mg-O compound group [39]. The summary band assignment is shown in Table 3.

Table 3. Band assignment of peel extract and MgO-NPs (Condition A)

	Wavenumber (cm ⁻¹)			
Band Assignment	Banana Peel Extract	Before	Calcined	Calcined
		Calcine	(600 °C)	(800 °C)
O-H stretch	3340.71	3308.85	3086.11	-
N-H stretch	3340.71	-	-	-
C-H stretch	-	2924.09 & 2854.65	-	-
O-H bend	1635.64	1620.21	-	-
C-H bend	-	1373.32	-	-
Mg-H	-	-	1404.18 & 1465.90	1427.32
C-O	-	1141.86	-	-
C-O-C	-	964.41	-	-
Mg-O	-	648.08	594.08	594.08

Similar FTIR results were obtained for MgO-NPs synthesized with Condition B, as shown in Figure 3. The broad peak centered at (a) 3340.71 cm⁻¹, (b) 3348.42 cm⁻¹, and (c) ,194.12 cm⁻¹ were due to the O-H stretch [18]. Also, the absorption peaks at (a) 1635.64 cm⁻¹ and (b) 1,627.92 cm⁻¹, which corresponded to the bending mode of O-H bonds which came from the hydroxyl groups of the phytochemicals of peel extract solution that were involved in the capping reaction [18,39].

Similarly, based on Figure 3 (b), Figure 3 (c) and Figure 3 (d), both O-H peaks became narrower and eventually disappeared with increasing calcination temperature when more water molecules were evaporated [40]. As mentioned, the broad peak centered at (a) 3340.71 cm⁻¹ could also be the stretching vibration of N-H groups

other than O-H groups. N-H groups are a feature of phenolic compounds, such as glycosides, tannins, and flavonoids [41] which agrees with the phytochemical test results of the extract.

Furthermore, the two small absorption peaks observed in Figure 3 (b) at 2924.09 cm⁻¹ and 2851.49 cm⁻¹ represented the C-H stretching vibration in CH₂ groups. This could be attributed to the phytochemical compounds [42]. As the calcination temperature increased, the peaks became increasingly indistinguishable. This indicated that the phytochemical compound capping reaction had taken place.

The C-H bending vibration is represented by the absorption peak at (b) 1334.74 cm⁻¹. The peaks at (c)

1411.89 cm⁻¹ – 1473.62 cm⁻¹ were attributed to Mg-H indicating the presence of hydride ion [44]. Besides, C-O and C-O-C diagnostic bonds were most likely responsible for absorption peaks between (b) 964.41 cm⁻¹, and 1141.86 cm⁻¹ [42]. When the samples were calcined, the peaks narrowed, indicating that the phytochemicals had undergone a capping reaction.

The extra peaks that appeared at 3194.12 cm⁻¹, 1473.62 cm⁻¹, 1411.80 cm⁻¹, 1056.99 cm⁻¹ and (d) 1049.28 cm⁻¹ could be because of: (1) the formation of crystalline inorganic compounds present in the extract solution

during the calcination process; and (2) strong bonds that stabilized the formation of MgO-NPs after the degradation of phytochemicals which remained over the surface of MgO-NPs [41].

Based on all the FTIR spectra obtained for green synthesized MgO-NPs with Condition B, the broad absorption peaks at (b) 655.80 cm⁻¹ and (c, d) 594.08 cm⁻¹ indicated the stretching vibration mode for the Mg-O compound group [39] which confirmed the production of MgO. The summary band assignment is shown in Table 4.

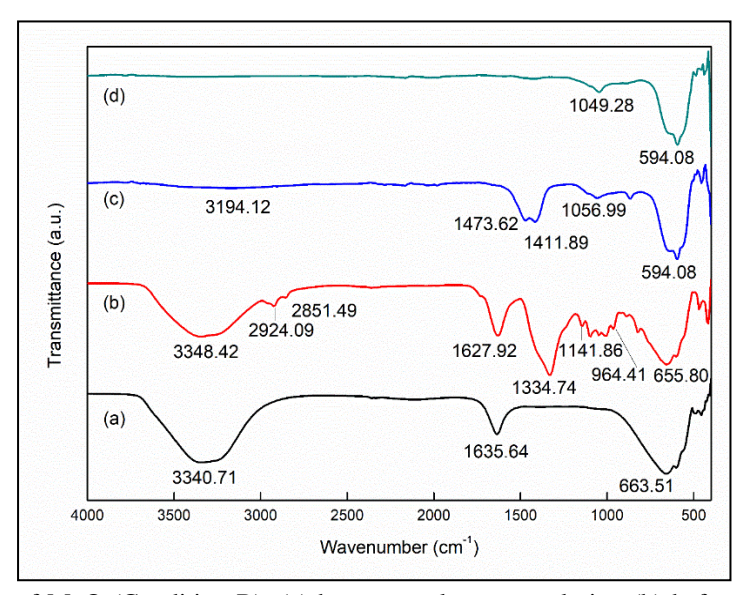


Figure 3. FTIR Spectra of MgO (Condition B): (a) banana peel extract solution (b) before calcine; (c) calcined at 600 °C; (d) calcined at 800 °C

Table 4. Band assignment of peel extract and MgO-NPs (Condition B)

	Wavenumber (cm ⁻¹)			
Band Assignment	Banana Peel Extract	Before	Calcined	Calcined
		Calcine	(600 °C)	(800 °C)
O-H stretch	3340.71	3348.42	3194.12	=
N-H stretch	3340.71	-	-	-
C-H stretch	-	2924.09 & 2851.49	-	-
O-H bend	1635.64	1627.92	-	-
C-H bend	-	1334.74	-	-
Mg-H	-	-	1411.89 & 1473.62	-
C-O	-	1141.86	-	-
C-O-C	-	964.41	-	-
Mg-O	-	655.80	594.08	594.08

Ultraviolet-Visible (UV-Vis) Spectroscopy

The synthesis of MgO-NPs was confirmed by the appearance of a maximum surface plasmon resonance (SPR) detected by UV-Vis spectroscopy. SPR located at different wavelengths can affect the shape, size and well distribution of green synthesized NPs [45].

The size of MgO-NPs produced through green synthesis tended to be small when the SPR band is located at wavelength lesser than 300 nm. However, the absorption peak shifted to larger wavelength (red-shift) with increasing particle size [46]. As shown in Figure 4, the absorption of the MgO-NPs synthesized with Condition A, calcined at 600 °C and 800 °C showed wavelengths at 264.50 nm and 265.50 nm, respectively. On the other hand, the absorption band of MgO-NPs formed with

Condition B (Figure 5) was located at wavelength 264 nm for both calcination temperatures (600 °C and 800 °C).

According to previous studies, the absorption of UV-Vis spectrum of MgO-NPs was reported between 260 nm—300 nm [18, 39, 42, 47, 48]. Therefore, the absorption peak of MgO-NPs obtained with both conditions were within the accepted wavelength range. This meant that, the change in concentration of Mg(NO₃)₂.6H₂O and volume of extract solution did not have a significant effect on the formation of MgO-NPs. However, MgO-NPs calcined at 800 °C showed a higher absorbance value indicating more yield of MgO-NPs [33]. This was due to the faster rate of crystal growth at higher temperature as thermal energy increased [49].

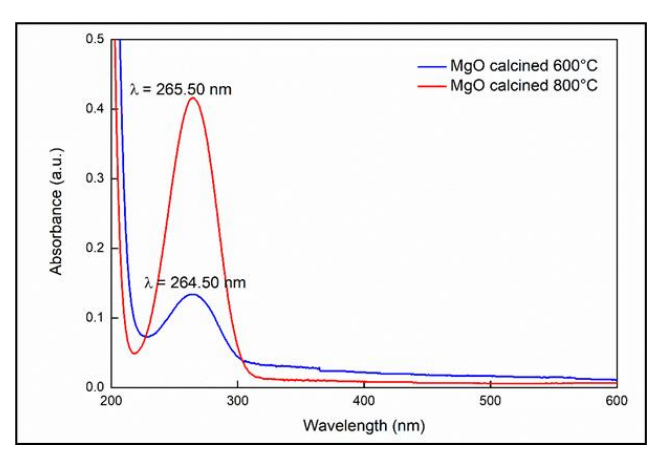


Figure 4. UV-Vis spectra of MgO-NPs (Condition A) calcined at 600 and 800 °C

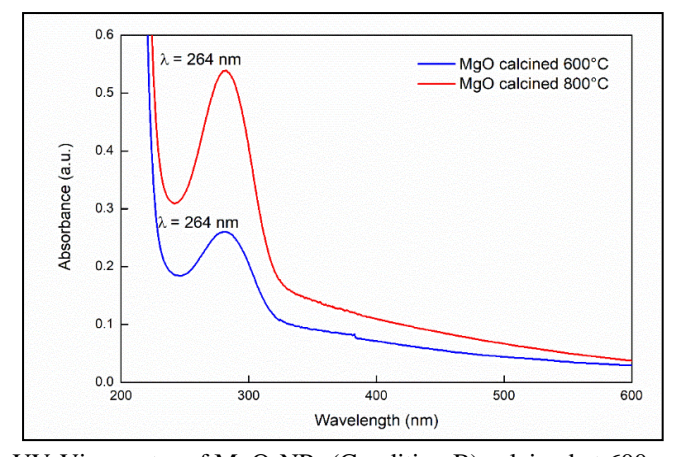


Figure 5. UV-Vis spectra of MgO-NPs (Condition B) calcined at 600 and 800 °C

Scanning electron microscope (SEM)

The morphology of the MgO-NPs is presented in Figure 6, Figure 7, Figure 8, and Figure 9. In general, the average particle size for MgO-NPs synthesized with Condition A and Condition B with different calcination temperatures varies. The products of green synthesis with Condition A, calcined at 600 °C and 800 °C, as well as products formed with Condition B, calcined at 600 °C were not within the nanoparticles size range. Whereas, the MgO-NPs produced with Condition B and calcined at 800 °C was within the nanoparticle size range of 1 nm – 100 nm [50]. The bigger particle size for MgO-NPs calcined was due to secondary phase, Mg(OH)₂, present in the MgO lattice causing it to be less crystalline [49]. This finding contradicts other study which stated that

higher calcination temperature increases the particle size. However, the study only studied the effect of calcination temperature while other conditions were kept constant [51].

Based on previous studies, the concentration and amount of extract used, reaction temperature, and pH value could affect the variable parameters, such as size, shape, and agglomeration [52, 53]. Figure 6 shows the SEM images of MgO-NPs synthesized with Condition A with calcination temperature of 600 °C. The particles had non uniform shape with an average size of 316.78 nm, the smallest particle was about 107 nm while the largest particle was about 550 nm with some degree of agglomeration.

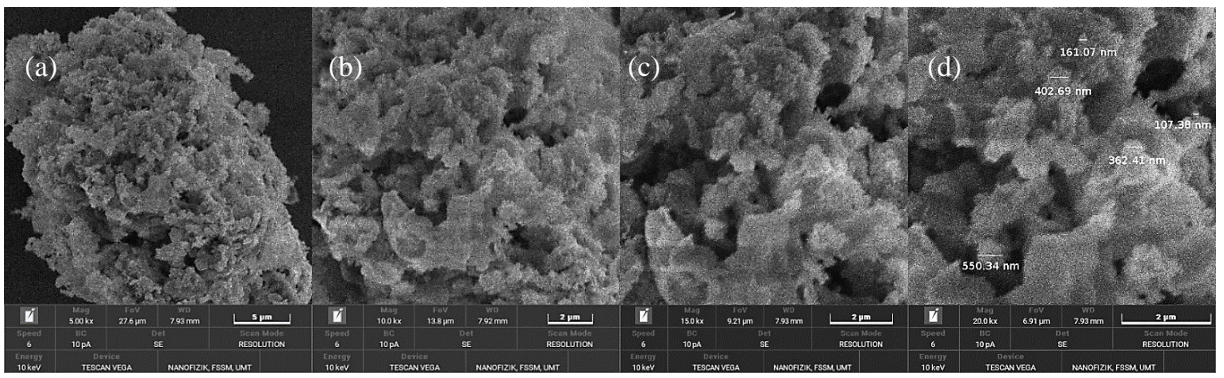


Figure 6. SEM images of MgO-NPs (Condition A) calcined at 600°C; at (a) 5,000x, (b) 10,000x, (c) 15,000x, and (d) 20,000x magnification

As shown in Figure 7, the particles synthesized with Condition A and calcined at 800 °C also had a non-uniform shape with an average size of 140.52 nm. The

smallest particle was about 62 nm while the largest particle was about 255 nm with some degree of agglomeration as well.

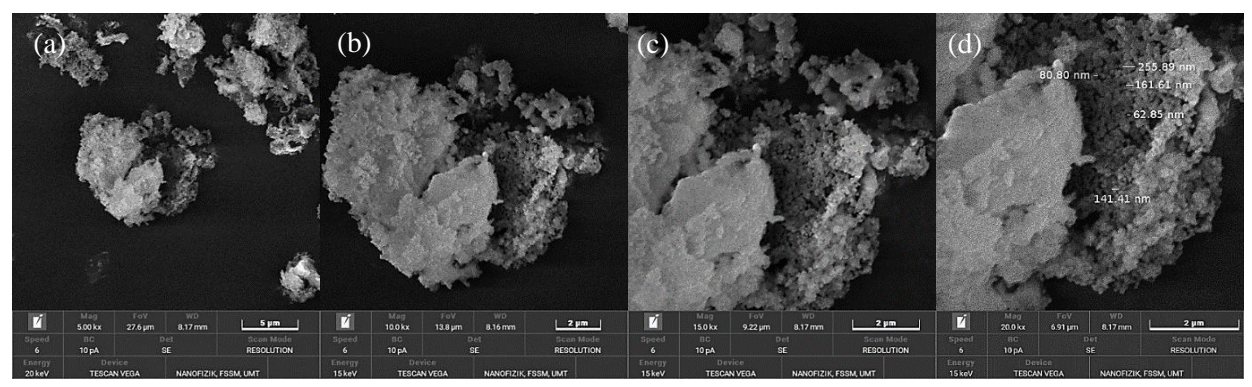


Figure 7. SEM images of MgO-NPs (Condition A) calcined at 800 °C; at (a) 5,000x, (b) 10,000x, (c) 15,000x, and (d) 20,000x magnification

Furthermore, Figure 8 shows the SEM images of synthesized MgO-NPs with Condition B and calcined at 600 °C. Most of the particles had irregular shapes with

a mean particle size of 208.31 nm. The smallest particle was around 148 nm, and the biggest particle was about 255 nm. Some degree of agglomeration was observed.

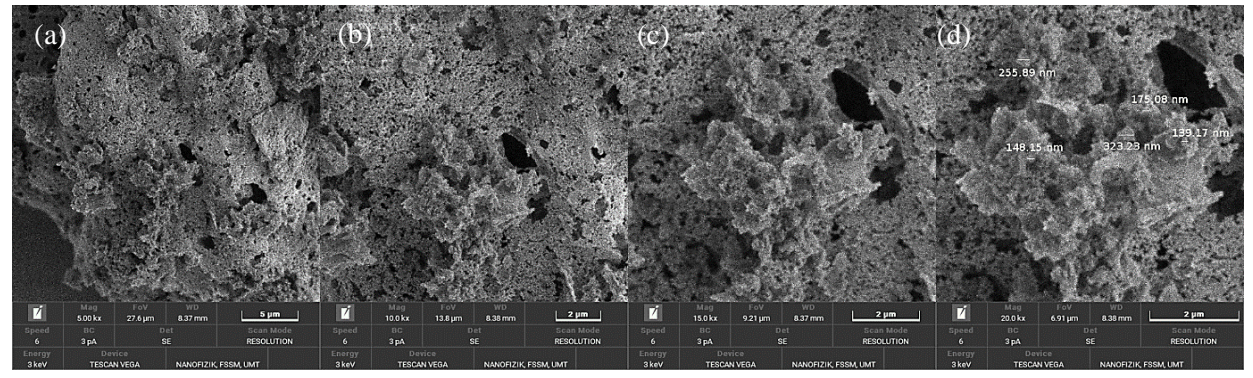


Figure 8. SEM images of MgO-NPs (Condition B) calcined at 600°C; at (a) 5,000x, (b) 10,000x, (c) 15,000x, and (d) 20,000x magnification

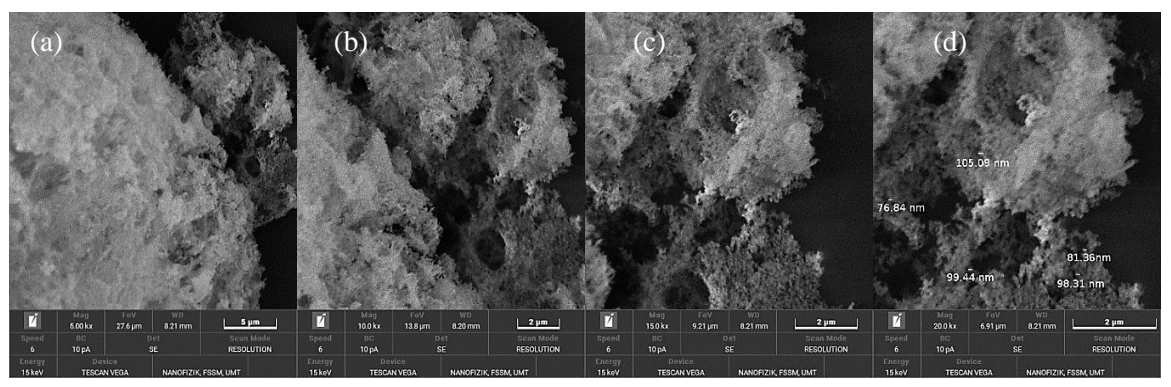


Figure 9. SEM images of MgO-NPs (Condition B) calcined at 800°C; at (a) 5,000x, (b) 10,000x, (c) 15,000x, and (d) 20,000x magnification

Lastly, Figure 9 shows the SEM images of MgO-NPs synthesized with Condition B and calcined at 800 °C. Most of the particles had non-uniform size and shapes with smaller crystallite as compared to other samples. The average particle size was 92.20 nm, with smallest particle of about 80 nm and largest particle of about 105 nm. Overall, all samples were highly agglomerated.

X-ray diffraction (XRD)

The synthesized MgO-NPs were subjected to x-ray diffraction analyses to confirm the presence and size of the NPs, obtain the crystallinity or amorphic nature, and detect possible impurities [41]. Figure 10 and Figure 11 show the x-ray diffraction pattern for MgO-NPs synthesized with Condition A and Condition B,

respectively. Based on the PDF reference card No.9000493, the MgO-NPs obtained were in cubic structure with space group Fm-3m (225). Similar results were obtained for MgO-NPs synthesized with Condition A and Condition B. All the peaks observed for the MgO-NPs as listed in Table 5 and Table 6 were also in agreement with the PDF reference card No.9000493 and previous studies [45,49,51].

The presence of MgO-NPs was confirmed as all the samples (calcined at 600 °C and 800 °C) showed the presence of peaks corresponding to (111), (200), (220), (311) and (222) planes. Other than that, the sharp characteristic peaks in the diffractogram indicated the highly crystalline structure of MgO-NPs [49]. The MgO

peaks became sharper as the calcination temperature increased as evidenced in the Figures and Tables.

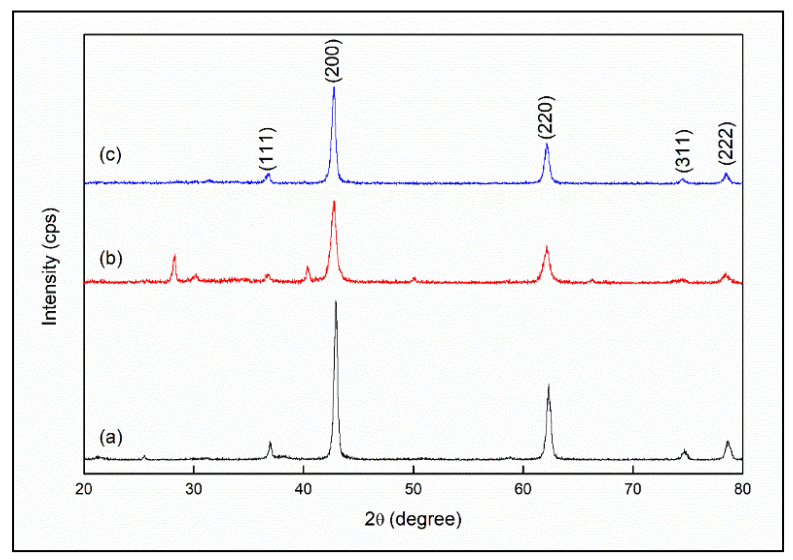


Figure 10. XRD of MgO-NPs (Condition A) (a) commercial and calcined at (b) 600 °C, and (c) 800 °C

Table 5. Crystallinity parameter of MgO-NPs synthesised with Condition A (a) Calcined at 600 °C

2θ (°)	β (°)	Intensity (cps)	Lattice Plane	Mean Particle size (nm)	
28.280	0.301	50	-	-	
30.17	0.48	12	-	-	
36.72	0.45	13	111	19.44	
40.40	0.33	30	-	-	
42.757	0.544	164	200	16.39	
49.991	0.19	13	-	-	
62.17	0.61	70	220	15.89	
66.30	0.41	6	-	-	
74.51	1.17	5	311	8.91	
78.34	0.78	15	222	13.73	
(b) Calo	(b) Calcined at 800 °C				

(b) Carefiled at 500 C					
2θ (°)	β (°)	Intensity (cps)	Lattice Plane	Mean Particle Size (nm)	
36.80	0.48	25	111	18.23	
42.736	0.414	290	200	21.53	
62.10	0.449	126	220	21.58	
74.45	0.41	16	311	25.43	
78.49	0.43	32	222	24.93	

However, several peaks corresponded to impurities were detected for the MgO-NPs calcined at 600 °C. The extra impurities peaks detected were caused by stable crystalline inorganic compounds formed during the

calcination of pre-calcine samples containing Mg(OH)₂ and strong bonds that remained over the surface of MgO-NPs [41]. On the other hand, no peaks other than the characteristic peaks of MgO were detected for the

MgO-NPs calcined at 800 °C, indicating that pure MgO-NPs were synthesized.

The average crystallite size of the MgO-NPs was estimated by using the Debye Scherrer's formula. When calcined at 600 °C, MgO-NPs synthesized with

Condition A were approximately 9 nm–20 nm, but when calcined at 800 °C, they were roughly 18 nm–25 nm. Besides, MgO-NPs synthesized by using Condition B had a diameter of 9 nm–20 nm when calcined at 600 °C and was 17 nm–23 nm when calcined at 800 °C.

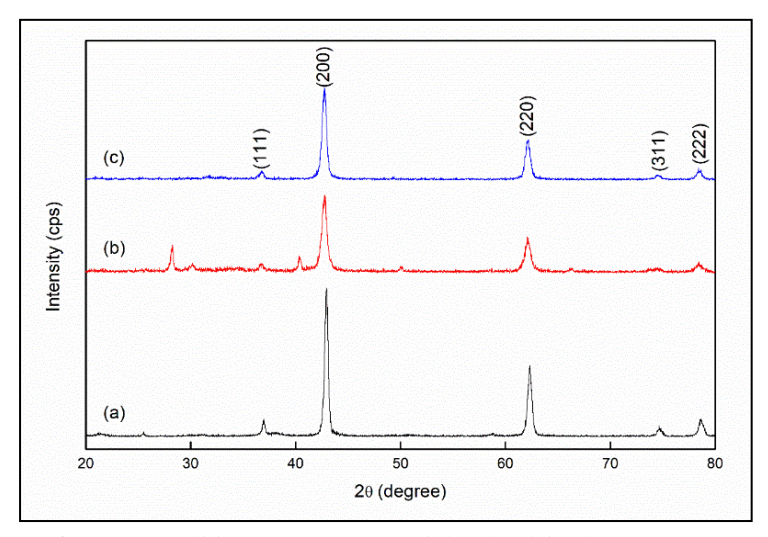


Figure 11. XRD of MgO (Condition B) (a) commercial and calcined at (b) 600 °C, and (c) 800 °C

Table 6. Crystallinity parameter of MgO nanoparticles synthesised with Condition B
(a) Calcined at 600 °C

(a) Call	(a) Calcined at 600 C					
2θ (°)	β (°)	Intensity (cps)	Lattice Plane	Mean Particle Size (nm)		
28.280	0.301	50	-	-		
30.17	0.48	12	-	-		
36.72	0.45	13	111	19.44		
40.40	0.33	30	-	-		
42.757	0.544	164	200	16.39		
49.991	0.19	13	-	-		
62.17	0.61	70	220	15.89		
66.30	0.41	6	_	-		
74.51	1.17	5	311	8.91		
78.34	0.78	15	222	13.73		

(b) Calcined at 800 °C

2θ (°)	β (°)	Intensity (cps)	Lattice Plane	Mean Particle Size (nm)
36.84	0.50	23	111	17.50
42.744	0.465	301	200	19.17
62.10	0.529	129	220	18.32
74.46	0.45	16	311	23.17
78.44	0.54	31	222	19.85

Conclusion

In summary, MgO-NPs have been successfully synthesized by using cavendish banana peel extract as reducing and capping agent, proving the concept of waste-to-wealth. The synthesis of MgO-NPs by using this banana peels with two methods of study which employed different volume of extracts and starting materials as well as different volume of starting materials were both reproducible as they both showed similar thermal stability. FTIR has shown that the mechanism of synthesis in this study were reduction and capping as the peaks of functional groups for biomolecules in the plants appeared in the pre-calcined samples for both methods. However, the peaks disappeared after calcination showing the occurrence of a full reduction and capping of the produced nanoparticles. Morphology and shapes of nanoparticles are dependent of the concentration and volume of starting materials, volume of extracts and calcination temperatures. As shown in SEM images, method A produced spherical shaped nanoparticles while method B produced irregular shaped nanoparticles. In the future, further research on the relationship between morphology of MgO-NPs and the properties of MgO-NPs can be studied in order to customizing the applications of MgO-NPs in the biological, physical and all nanotechnology-related fields. Overall, the best results obtained were from Condition B (25 mL extract with 0.1 M concentration of starting materials), thus sustainable and optimized synthesis methods have been successfully developed for future exploration of MgO-NPs. More waste products can be explored in the future providing more sustainable resources of reducing agent for the synthesis of MgO-NPs.

Acknowledgement

Authors would like to thank Universiti Malaysia Terengganu for providing funding support for this project (UMT/TAPE-RG/2021/55338) and Faculty of Science and Marine Environment for providing the logistical support including the laboratory and needed instruments in completing this study.

References

1. United States Environmental Protection Agency (2023). Basics of green chemistry.

- https://www.epa.gov/greenchemistry/basics-greenchemistry [Accessed on 17 July 2023].
- Murcia, J. E., Martinez, S., Martins V., Herrera, D., Buitrago, C., Velasquez, A., Ruiz, F. and Torres, M. (2023). Risk assessment and green chemistry applied to waste generated in university laboratories. *Heliyon*, 9(5): e15900.
- 3. Khandel, P., Yadaw, R. K., Soni, D. K., Kanwar, L. and Shahi, S. K. (2018). Biogenesis of metal nanoparticles and their pharmacological applications: present status and application prospects. *Journal of Nanostructure in Chemistry*, 8(3): 217-254.
- Kumar, P. P., Bhatlu, M. L. D., Sukanya, K., Karthikeyan, S, and Jayan, N. (2020). Synthesis of magnesium oxide nanoparticle by eco-friendly method (green synthesis)—A review. *Materials Today: Proceedings*, 37: 3028-3030.
- Singh, J., Dutta, T., Kim, KH., Rawat, M., Samdar, P. and Kumar, P. (2018). 'Green' synthesis of metals and their oxide nanoparticles: applications for environmental remediation. *Journal of Nanobiotechnology*, 16(1): 84.
- Narendhran, S., Manikandan, M. and Shakila, P. B. (2019). Antibacterial, antioxidant properties of *Solanum trilobatum* and sodium hydroxide-mediated magnesium oxide nanoparticles: a green chemistry approach. *Bulletin of Materials Science*, 42(3): 1-8.
- Ganapathi Rao, K., Ashok, C. H., Venkateswara Rao, K., Shilpa Chakra, C. H. and Akshaykranth, A. (2015). Eco-friendly synthesis of MgO nanoparticles from orange fruit waste. *International Journal Advance Research Physical Science*, 2: 1-6.
- 8. Vishwasrao, C., Momin, B. and Ananthanarayan, L. (2019). Green synthesis of silver nanoparticles using sapota fruit waste and evaluation of their antimicrobial activity. *Waste and Biomass Valorization*, 10(8): 2353-2363.
- 9. Farani R. M., Farsadrooh, M., Zare, I., Gholami, A. and Akhavan, O. (2023). Green synthesis of magnesium oxide nanoparticles and nanocomposites for photocatalytic antimicrobial, antibiofilm and antifungal applications. *Catalysts*, 13(4): 642.

- Chaudhary, J., Tailor, G., Yadav, M., and Mehta, C. (2023). Green route synthesis of metallic nanoparticles using various herbal extracts: A review. *Biocatalysis and Agricultural Biotechnology*, 50: 102692.
- 11. Ramanujam, K., and Sundrarajan, M. (2014). Antibacterial effects of biosynthesized MgO nanoparticles using ethanolic fruit extract of *Emblica officinalis*. *Journal of Photochemistry and Photobiology B: Biology*, 141: 296-300.
- 12. Moorthy, S. K., Ashok, C. H., Rao, K. V., and Viswanathan, C. (2015). Synthesis and characterization of MgO nanoparticles by neem leaves through green method. *Materials Today: Proceedings*, 2(9): 4360-4368.
- 13. Umaralikhan, L., and Jamal Mohamed Jaffar, M. (2018). Green synthesis of MgO nanoparticles and its antibacterial activity. *Iranian Journal of Science and Technology, Transaction A: Science*, 42(2): 477-485.
- 14. Dabhane, H., Ghotekar, S., Zate, M., Kute, S., Jadhav, G. and Medhane, V. (2022). Green synthesis of MgO nanoparticles using aqueous leaf extract of Ajwain (*Trachyspermum ammi*) and evaluation of their catalytic and biological activities. *Inorganic Chemistry Communications*, 138: 109270.
- Duong, T. H. Y., Nguyen, T. N., Oanh, H. T., Dang Thi, T. A., Giang, L. N. T., Phuong, H. T., Anh, N. T., Nguyen, B. M., Quang, V. T., Le, G. T. and Nguyen, T. van. (2019). Synthesis of magnesium oxide nanoplates and their application in nitrogen dioxide and sulfur dioxide adsorption. *Journal of Chemistry*, 2019: 4376429.
- Suresh, J., Yuvakkumar, R., Sundrarajan, M., and Hong, S. I. (2014). Green synthesis of magnesium oxide nanoparticles. *Advanced Materials Research*, 952: 141-144.
- Ali, R., Shanan, Z. J., Saleh, G. M., and Abass, Q. (2020). Green synthesis and the study of some physical properties of MgO nanoparticles and their antibacterial activity. *Iraqi Journal of Science*, 61(2): 266-276.
- Vijayakumar, S., Punitha, V. N., and Parameswari, N. (2021). Phytonanosynthesis of MgO nanoparticles: Green synthesis, characterization and antimicrobial evaluation. *Arabian Journal for*

- Science and Engineering, 2021: 1-6.
- Prasanth, R., Kumar, S. D., Jayalakshmi, A., Singaravelu, G., Govindaraju, K. and Kumar, V. G. (2019). Green synthesis of magnesium oxide nanoparticles and their antibacterial activity. *Indian Journal of Geo Marine Sciences*, 48(8): 1210-1215.
- 20. Amina, M., al Musayeib, N. M., Alarfaj, N. A., El-Tohamy, M. F., Oraby, H. F., Al Hamoud, G. A., Bukhari, S. I., and Moubayed, N. M. S. (2020). Biogenic green synthesis of MgO nanoparticles using *Saussurea costus* biomasses for a comprehensive detection of their antimicrobial, cytotoxicity against MCF-7 breast cancer cells and photocatalysis potentials. *PLoS ONE*, 15: 0237567.
- 21. Balakrishnan, G., Velavan, R., Mujasam Batoo, K., and Raslan, E. H. (2020). Microstructure, optical and photocatalytic properties of MgO nanoparticles. *Results in Physics*, 16: 103013.
- 22. Ammulu, M. A., Vinay Viswanath, K., Giduturi, A. K., Vemuri, P. K., Mangamuri, U. and Poda, S. (2021). Phytoassisted synthesis of magnesium oxide nanoparticles from *Pterocarpus marsupium* rox.b heartwood extract and its biomedical applications. *Journal of Genetic Engineering and Biotechnology*, 19: 21.
- 23. Pugazhendhi, A., Prabhu, R., Muruganantham, K., Shanmuganathan, R. and Natarajan, S. (2019). Anticancer, antimicrobial and photocatalytic activities of green synthesized magnesium oxide nanoparticles (MgONPs) using aqueous extract of Sargassum wightii. *Journal of Photochemistry and Photobiology B: Biology*, 190: 86-97.
- 24. Cai, L., Chen, J., Liu, Z., Wang, H., Yang, H. and Ding, W. (2018). Magnesium oxide nanoparticles: Effective agricultural antibacterial agent against *Ralstonia solanacearum*. *Frontiers in Microbiology*, 9: 790.
- 25. Chandrasekar, M., Subash, M., Perumal, V., Panimalar, S., Aravindan, S., Uthrakumar, R., Inmozhi, C., Isaev, A. B., Muniyasamy, S., Raja, A. and Kaviyarasu, K. (2022). Specific charge separation of Sn doped MgO nanoparticles for photocatalytic activity under UV light irradiation. Separation and Purification Technology, 2021: 294.
- 26. Pandit, C., Roy, A., Ghotekar, S., Khusro, A., Islam, M. N., Emran, T. bin, Lam, S. E., Khandaker, M. U.

- and Bradley, D. A. (2022). Biological agents for synthesis of nanoparticles and their applications. *Journal of King Saud University Science*, 34(3): 101869.
- 27. Marfu'ah, S., Rohma, S. M., Fanani, F., Hidayati, E. N., Nitasari, D. W., Primadi, T. R., Ciptawati, E., Sumari, S., and Fajaroh, F. (2020, May). Green synthesis of ZnO nanoparticles by using banana peel extract as capping agent and its bacterial activity. 2nd International Conference on Chemistry and Material Science (IC2MS), 833: 1-7.
- 28. Naganathan, S. and Thirunavukkarasu, S. (2017). Green way genesis of silver nanoparticles using multiple fruit peels waste and its antimicrobial, antioxidant, and anti-tumor cell line studies. 2nd International Conference on Mining, Material and Metallurgical Engineering, 191: 1-7.
- 29. Abdullah, F. H., Abu Bakar, N. H. H. and Abu Bakar, M. (2020). Low temperature biosynthesis of crystalline zinc oxide nanoparticles from Musa acuminata peel extract for visible-light degradation of methylene blue. *Optik*, 206: 164279.
- 30. Abdullah, F. H., Abu Bakar, N. H. H. and Abu Bakar, M. (2021). Comparative study of chemically synthesized and low temperature bio-inspired Musa acuminata peel extract mediated zinc oxide nanoparticles for enhanced visible-photocatalytic degradation of organic contaminants in wastewater treatment. *Journal of Hazardous Materials*, 406: 164279.
- 31. Hussien, N. A. (2023). Antimicrobial potential of biosynthesized zinc oxide nanoparticles using banana peel and date seeds extracts. *Sustainability* (*Switzerland*), 15(11): 9048.
- 32. Hussien, N. A., al Malki, J. S., al Harthy, F. A. R., Mazi, A. W. and Al Shadadi, J. A. A. (2023). Sustainable eco-friendly synthesis of zinc oxide nanoparticles using banana peel and date seed extracts, characterization, and cytotoxicity evaluation. *Sustainability*, 15(13): 9864.
- Shittu, H. O., Igiehon, E., Eremwanarue, A. O., Oijagbe, R. E., Momoh, M. O. and Agbontian, M. A. (2021). Optimization of phytosynthesis of magnesium oxide and magnesium chloride nanoparticles. *Nigerian Journal of Biotechnology*, 37(2): 74-83.

- 34. Vu, H. T., Scarlett, C. J. and Vuong, Q. V. (2018). Phenolic compounds within banana peel and their potential uses: A review. *Journal of Functional Foods*, 40: 238-248.
- 35. Gillani, S. F., Ali, S., Tahir, H. M., Shakir, H. A. and Hassan, A. (2020). Phytochemical analysis, antibacterial and antibiogram activities of fruits peels against human pathogenic bacteria. *International Food Research Journal*, 27(5): 963-970.
- 36. Nguyen, V. T., and Le, M. D. (2018). Influence of various drying conditions on phytochemical compounds and antioxidant activity of carrot peel. *Beverages*, 4(4): 80.
- 37. Saikumari, N., Dev, S. M., and Dev, S. A. (2021). Effect of calcination temperature on the properties and applications of bio extract mediated titania nano particles. *Scientific Reports*, 11(1): 1-17.
- 38. Kumar, S. A., Jarvin, M., Inbanathan, S. S. R., Umar, A., Lalla, N. P., Dzade, N. Y., Algadi, H., Rahman, Q. I. and Baskoutas, S. (2022). Facile green synthesis of magnesium oxide nanoparticles using tea (*Camellia sinensis*) extract for efficient photocatalytic degradation of methylene blue dye. *Environmental Technology and Innovation*, 28: 102746.
- 39. Essien, E. R., Atasie, V. N., Oyebanji, T. O. and Nwude, D. O. (2020). Biomimetic synthesis of magnesium oxide nanoparticles using *Chromolaena odorata* (L.) leaf extract. *Chemical Papers*, 1-9.
- 40. Yusoff, H. M., Idris, N.H., Hipul, N. F., Yusoff, N. F. M., Izham, N. Z. M. and Bhat, I. U. H. (2020). Green synthesis of zinc oxide nanoparticles using black tea extract and its potential as anode material in sodium-ion batteries. *Malaysian Journal of Chemistry*, 22(2): 43-51.
- 41. Hii, Y. S., Jeevanandam, J. and Chan, Y. S. (2019). Plant mediated green synthesis and nanoencapsulation of MgO nanoparticle from *Calotropis gigantea*: Characterisation and kinetic release studies. *Inorganic and Nano-Metal Chemistry*, 48(12): 620-631.
- 42. Essien, E. R., Atasie, V. N., Okeafor, A. O. and Nwude, D. O. (2020). Biogenic synthesis of magnesium oxide nanoparticles using *Manihot*

- esculenta (Crantz) leaf extract. International Nano Letters, 10(1): 43-48.
- 43. Latha, C. K., Raghasudha, M., Aparna, Y., Ramchander, M., Ravinder, D., Jaipal, K., Veerasomaiah, P. and Shridhar, D. (2017). Effect of capping agent on the morphology, size and optical properties of In₂O₃ nanoparticles. *Materials Research*, 20(1): 256-263.
- 44. Yusoff, H. M., Hazwani, N. U., Hassan, N. and Izwani, F. (2015). Comparison of sol gel and dehydration magnesium oxide (MgO) as a catalyst in Michael addition reaction. *International Journal of Integrated Engineering*, 7(3): 43-50.
- 45. Hassan, S. E. D., Fouda, A., Saied, E., Farag, M., Eid, A. M., Barghoth, M. G. and Awad, M. F. (2021). Rhizopus Oryzae-mediated green synthesis of magnesium oxide nanoparticles (MgO-NPs): A promising tool for antimicrobial, mosquitocidal action, and tanning effluent treatment. *Journal of Fungi*, 7(5): 372.
- Osuntokun, J., Onwudiwe, D. C. and Ebenso, E. E. (2019). Green synthesis of ZnO nanoparticles using aqueous *Brassica oleracea* L. var. italica and the photocatalytic activity. *Green Chemistry Letters and Reviews*, 12(4): 444-457.
- 47. Dobrucka, R. (2018). Synthesis of MgO nanoparticles using Artemisia abrotanum herba extract and their antioxidant and photocatalytic properties. *Iranian Journal of Science and Technology, Transactions A: Science*, 42(2): 547-555.
- 48. Vidhya, E., Vijayakumar, S., Nilavukkarasi, M.,

- Punitha, V. N., Snega, S., and Praseetha, P. K. (2021). Green fabricated MgO nanoparticles as antimicrobial agent: Characterization and evaluation. *Materials Today: Proceedings*, 45: 5579-5583.
- 49. Farizan, A. F., Yusoff, H. M., Badar, N., Bhat, I. U. H., Anwar, S. J., Wai, C. P., Asari, A., Kasim, M. F., and Elong, K. (2023). Green synthesis of magnesium oxide nanoparticles using Mariposa *Christia vespertilionis* leaves extract and its antimicrobial study toward *S. aureus* and *E. coli. Arabian Journal for Science and Engineering*, 48(6): 7373-7386.
- 50. Adamo, G., Campora, S. and Ghersi, G. (2017). Nanostructures for novel therapy: synthesis, characterization and applications. Elsevier, Amsterdam: pp. 57-80.
- 51. Venkatachalam, A., Jesuraj, J. P., and Sivaperuman, K. (2021). *Moringa oleifera* leaf extract-mediated green synthesis of nanostructured alkaline earth oxide (MgO) and its physicochemical properties. *Journal of Chemistry*, 2021: 4301504.
- 52. Rahmani-Nezhad, S., Dianat, S., Saeedi, M., and Hadjiakhoondi, A. (2017). Synthesis, characterization and catalytic activity of plant mediated MgO nanoparticles using *Mucuna* pruriens L. seed extract and their biological evaluation. *Journal of Nanoanalysis*, 4(4): 290-298.
- Zhang, D., Ma, X. L., Gu, Y., Huang, H., and Zhang,
 G. W. (2020). Green synthesis of metallic nanoparticles and their potential applications to treat cancer. *Frontiers in Chemistry*, 8(799): 1-18.